Next generation battery salt sourcing—the example of calcium bis(fluorosulfonyl)imide (Ca(FSI)2)

JPhys Energy

PURPOSE-LED PUBLISHING™

PAPER • OPEN ACCESS

Next generation battery salt sourcing—the example of calcium bis(fluorosulfonyl)imide ($Ca(FSI)_2$)

To cite this article: Johanna Timhagen *et al* 2026 *J. Phys. Energy* **8** 015036

Journal of Physics: Energy

OPEN ACCESS

RECEIVED
11 December 2025

REVISED
5 March 2026

ACCEPTED FOR PUBLICATION
18 March 2026

PUBLISHED
27 March 2026

PAPER

Next generation battery salt sourcing—the example of calcium bis(fluorosulfonyl)imide ($Ca(FSI)_2$)

Johanna Timhagen[1], **Jonathan Weidow**[1] and **Patrik Johansson**[1,2,3,*]

[1] Department of Physics, Chalmers University of Technology, 412 96 Gothenburg, Sweden
[2] ALISTORE-European Research Institute, CNRS FR 3104, Hub de l'Energie, 80039 Amiens, France
[3] Department of Chemistry—Ångström, Uppsala University, 751 21 Uppsala, Sweden
[*] Author to whom any correspondence should be addressed.

E-mail: patrik.johansson@kemi.uu.se

Keywords: calcium metal batteries, Ca ion batteries, multivalent batteries, salt purity, commercial salt

Supplementary material for this article is available online

Abstract

High and uniform quality of commercially sourced materials is crucial for establishing trust and comparability across scientific studies. This is particularly true in the area of next generation batteries, as low-quality materials could wrongfully discourage a technology/chemistry from future use. Electrolyte salts are a class of materials that have historically been laden with such problems. Herein, the basic properties and performance of five commercial $Ca(FSI)_2$ salts are compared, focusing on thermal stability and phase transitions, along with vibrational spectroscopy techniques to assess the purity of the salts. Calcium battery electrolytes are prepared by dissolving the salts in dimethylacetamide and subsequently tested in both symmetric (Ca||Ca) and full cells (Ca||PTCDI). Notably, there are quite some differences between fundamental basic properties between all the five $Ca(FSI)_2$ salts, however, this is not really reflected in their electrochemical performance, which could be interpreted as rather reassuring. Nevertheless, it must be stressed that the differences may also be electrochemically significant for other calcium battery (electrolyte) designs and/or operating conditions.

1. Introduction

The advancement of next generation batteries (NGBs) depends on several factors, such as progress in terms of energy density [1], sustainability [2], *etc*, but also on prospects of long-term stable cycling and a proper understanding of mechanisms to, *e.g.* avoid electrolyte decomposition that shortens the lifetime [3]. The NGB technology of calcium batteries (CaBs) has steadily gained more research attention over the last decade [4, 5]. And for the theoretically most performant CaBs, *i.e.* Ca metal batteries (CMBs) [6, 7], one of the most critical obstacles is the calcium metal anode's propensity to form passivation layers—a phenomenon heavily influenced by the electrolyte chemistry and its degradation [8].

The first electrolyte to enable Ca plating and stripping was $Ca(BF_4)_2$ in EC:PC, albeit at elevated temperature [9]. However, commercial $Ca(BF_4)_2$ is sold as a hydrate and is notoriously difficult to dry properly [10]. The current gold standard of Ca-salts today is rather $Ca[B(hfip)_4]_2$ [11, 12], which has demonstrated reversible Ca plating and stripping in numerous solvents [13, 14]. However, $Ca[B(hfip)_4]_2$ is not yet commercially available, making it difficult to use as a common basis for CaB development. High-quality commercially readily available Ca-salts are central for the latter, and one such candidate, building on the previous success of the Li-salt analogue [15, 16], is calcium bis(fluorosulfonyl)imide ($Ca(FSI)_2$). As a fluorinated anion with a delocalized negative charge, FSI is commonly used in batteries for its chemical and thermal stability [15]. $Ca(FSI)_2$ has, however, in contrast to LiFSI, been sparsely used for CaBs [17–19], and relevant data are often reduced to supplementary information [20–22]. Calcium bis(trifluoromethanesulfonyl)imide ($Ca(TFSI)_2$), which is structurally very similar to $Ca(FSI)_2$,

has been used more frequently [20, 23, 24], and shown to render lower overpotentials, ascribed to a higher cation–anion dissociation degree [20].

Ten years ago, one of us published a study on the quality of commercially available LiFSI salts [25]. At that point, LIBs were already an established technology, but high and uniform quality of commercial Li-salts was highlighted in terms of establishing trust and comparability across scientific papers. In contrast, for CaBs, low and/or variable quality salts could impede the very development of a battery technology in its infancy. In this work, the thermal stability of five commercially sourced $Ca(FSI)_2$ salts was first characterized by monitoring degradation and phase transitions using both dynamic and isothermal thermal gravimetric analysis (TGA) as well as differential scanning calorimetry (DSC). Subsequently, detailed Raman and Fourier-transform infrared (FT-IR) spectroscopic analyses were made to address the purity of the salts. Finally, the impact of salt purity on the electrochemical performance was assessed using both symmetric and full CMB cells.

2. Experimental

2.1. Sample handling and preparation

Five $Ca(FSI)_2$ salts (hereafter 'A–E'), all commercially sourced, were dried, stored, and handled in an argon-filled glove box ($H_2O < 1$ ppm, $O_2 < 1$ ppm). The salts were dried in a vacuum Büchi oven (<7 Pa and 72 h at 70 °C). When dried, salts A and E are fine, dusty powders mixed with small agglomerates that can be lightly pressed into the same fine powder (figure S1). Salt B had a damp, fluffy texture as received, which, after drying, turned into the same dusty powder style as A and E. Salts C and D had a more granular appearance, and salt C, in particular, is very flaky. All salts, including the as-received version of salt B, had water contents low enough not to be detectable (<10 ppm) by Karl Fischer titration (KF Coulometer, Metrohm).

For the electrochemical tests, appropriate amounts of $Ca(FSI)_2$ were added to DMAc (Sigma-Aldrich, ReagentPlus®, ⩾99%, dried with 3 Å molecular sieves) to create 0.1 M $Ca(FSI)_2$ in DMAc electrolytes. Ca metal foils (ACI Alloys, 99.5% purity, 0.25 mm thickness) were polished using a Dremel® 8260 rotary tool equipped with a silicon carbide tip and further scraped with a stainless-steel spatula right before cell assembly, to avoid native passivation layers. Perylene-3,4,9,10-tetracarboxylic diimide (PTCDI, Tokyo Chemical Industry) based cathodes were created from a slurry prepared using 1-methyl-2-pyrrolidone (NMP, anhydrous, 99.5%, Sigma-Aldrich) and poly(vinylidene fluoride) (PVdF, Sigma-Aldrich) at a 70:20:10 PTCDI:NMP:PVdF ratio, mixed for several minutes until the desired slurry consistency was achieved, and then cast onto copper foil (Goodfellow GmbH, 0.1 mm thickness).

2.2. DSC

DSC was performed using a Q1000 from TA Instruments. Approximately 5–10 mg of sample was hermetically sealed in an aluminum pan. Here we use the methodology of [25]; the samples were cooled at a rate of 10 °C min^{-1} to −100 °C, isothermally maintained for 5 min, and then heated at a rate of 5 °C min^{-1}–280 °C. The onsets of the exothermal phase transitions were used to determine the solid–solid transition points (T_{s-s}) and the onsets of the endothermal phase transitions were used to determine the melting points (T_m).

2.3. TGA

TGA was performed using a TG209 F1 Iris from Netzsch. Approximately 5–10 mg of sample was hermetically sealed in an aluminum pan, with a pinhole in the lid to permit gases to be released. The following TGA programs both used the methodology of ref. 25. All samples were heated from 25 °C to 500 °C at a rate of 5 °C min^{-1}. The decomposition temperatures (T_d) were defined as the temperature at which 1% and 5% mass loss have occurred. Additionally, isothermal TGA measurements were performed at 100 °C and 125 °C to study long-term stability. At each temperature, the measurements were maintained for 12 h, followed by a dynamic step with a heating rate of 5 °C min^{-1}–500 °C.

2.4. Raman spectroscopy

Raman data were recorded with a Bruker MultiRAM FT-Raman spectrometer, featuring a spectral resolution of 2 cm^{-1} and an Nd:YAG laser (1064 nm, 300 mW) as the excitation source. The data were averaged over 4000 scans and recorded at room temperature. Here we use the methodology of [25], but with a considerably larger amount of scans. All samples were ground into fine powder with a mortar and pestle, and then filled and sealed in glass vials inside an argon-filled glove box.

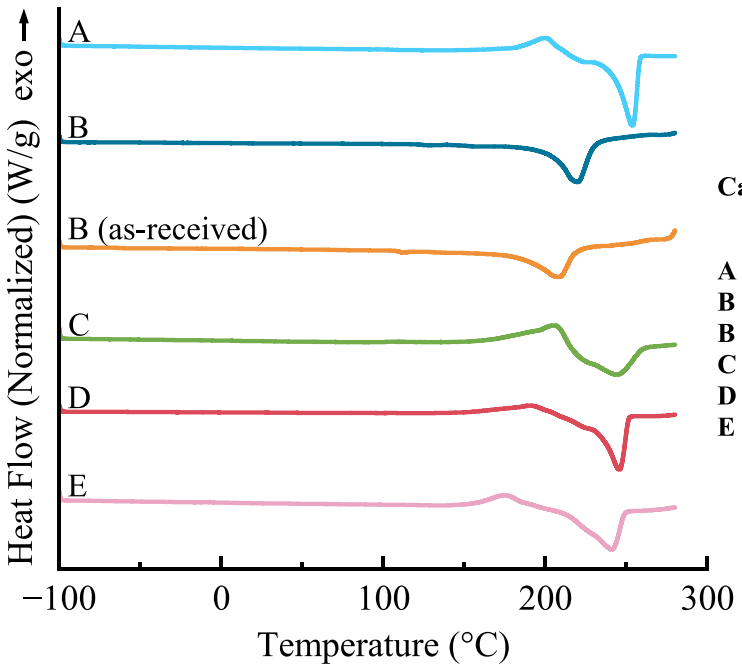

$Ca(FSI)_2$	Exotherm [°C]	T_m [°C]
A	199	240
B		205
B (as-received)		189
C	205	213
D	190	231
E	175	215

Figure 1. DSC heating traces of $Ca(FSI)_2$ salts A–E and corresponding event temperatures.

2.5. FT-IR spectroscopy

An attenuated total reflection Alpha FT-IR spectrometer from Bruker, with a diamond crystal as the refractive element and positioned inside the glove box, was used to record the IR spectra. The methodology of ref. 25 was used, but with a considerably larger amount of scans. The samples and background were measured using 120 scans each. Data were collected at 28 °C between 400 and 4000 cm^{-1} using a resolution of 2 cm^{-1}. Proper contact between the samples and the diamond crystal was assured by applying pressure with the module piston.

2.6. Electrochemical testing

Coin cells were assembled inside the glove box. Both symmetric Ca||Ca cells and full cells were made using a glass microfiber separator (Whatman® paper) soaked with 60 μl 0.1 M $Ca(FSI)_2$ in DMAc electrolyte. Symmetric cells were cycled at a current density of 0.02 mA cm^{-2} until failure, and the rate capability was tested at a constant areal capacity of 0.02 mAh cm^{-2}. The Ca||PTCDI full cells were cycled at a C/5 rate (1 °C = 137 mAh g^{-1}) in the potential window of 0.5–3.0 V *vs* $Ca^{2+}/Ca°$.

3. Results and discussion

First, the phase and thermal stabilities of the salts were monitored, whereafter they were spectroscopically investigated in terms of purity. Finally, electrolytes based on salts A–E were used in electrochemical cells.

3.1. Phase transitions

The DSC heating traces show both similarities and differences across the salts A–E (figure 1). While salts A and C–E show exothermal events at rather similar temperatures, salt B notably, both as-received and dried, shows no such events, but instead melts at approximately the same temperature, which furthermore is *ca.* 10 °C–50 °C before the other salts melt. For LiFSI, which melts at 137 °C [25], its endothermal melting peak has been shown to reduce in depth, and even become exothermal with increasing water content [26], and it can cautiously be suggested that $Ca(FSI)_2$ would behave similarly. However, if so, this would most likely push the exothermal event to higher temperatures, as the divalent Ca^{2+} cation coordinates both water and anions more strongly. Yet, with very low water content, this is much more likely a solid–solid phase transition.

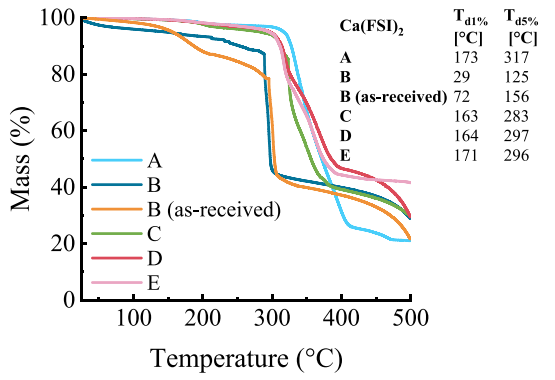

Figure 2. Dynamic TGA of $Ca(FSI)_2$ salts A–E and corresponding decomposition temperatures.

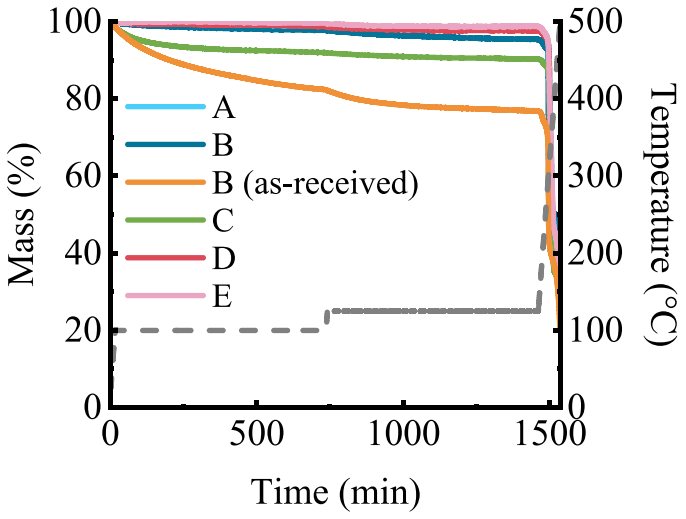

Ca(FSI)2	Mass loss [%] after 12 h at 100 °C	Mass loss [%] after 12 h at 125 °C
A	1.2	1.7
B	2.3	4.6
B (as-received)	17.6	23.2
C	8.0	10.0
D	1.3	2.4
E	0.4	1.2

Figure 3. Isothermal TGA of $Ca(FSI)_2$ salts A–E and corresponding mass losses.

3.2. Thermal stability

The dynamic TGA data show that salts A and C–E all decompose at 168 ± 5 °C (figure 2)—hence before the exothermal events in the DSC traces if the very strict $T_{d1\%}$ measure is used. The $T_{d5\%}$ measure, in contrast, yields decomposition temperatures in the range of 283 °C–317 °C, indicating no significant mass losses prior to solid–solid phase transition and subsequent melting. Salt B is again very different; dried, it decomposes already at 29 °C ($T_{d1\%}$) and at 125 °C ($T_{d5\%}$), and as-received, at 72 °C ($T_{d1\%}$) and 156 °C ($T_{d5\%}$). This leads us to suspect that it is still hydrated, despite the Karl-Fisher measurement, and perhaps also partially decomposes during the drying process itself. Moreover, the residual masses remaining at 500 °C provide further indications of differences—either in composition or possibly in how the salts granularity *etc.* affects the data, this as salt A and the as-received version of salt B exhibit ∼20%, salts B–D ∼30%, and salt E ∼40% residual masses.

A different trend in thermal stability is obtained from isothermal TGA, where salts A, D, and E lose very little mass both at 100 °C and after the additional 12 h at 125 °C (figure 3). The dried salt B has only a slightly greater mass loss, in fact, less than in dynamic TGA at the same temperatures. As salt B in its as-received state loses significantly more mass, it is reasonable to assume that it loses significant mass during drying. While this might not have been water, any contamination is equally concerning. Finally, salt C also loses a considerable amount of mass in the isothermal TGA, which is particularly worrying, given that this occurs *after* drying. The analogous LiFSI, which is synthesized first by producing the FSI anion and then introducing the Li cation, has impurities from the FSI step in the form of $NH_4H_SO_4$, HCl, CO_2, and $POCl_3$, and/or from metal ions from SbF_3, KF, ZnF_2, and AlF_3[15]. Assuming that the synthesis of FSI is analogous, the impurities of LiFSI and $Ca(FSI)_2$ are most likely the very same as well.

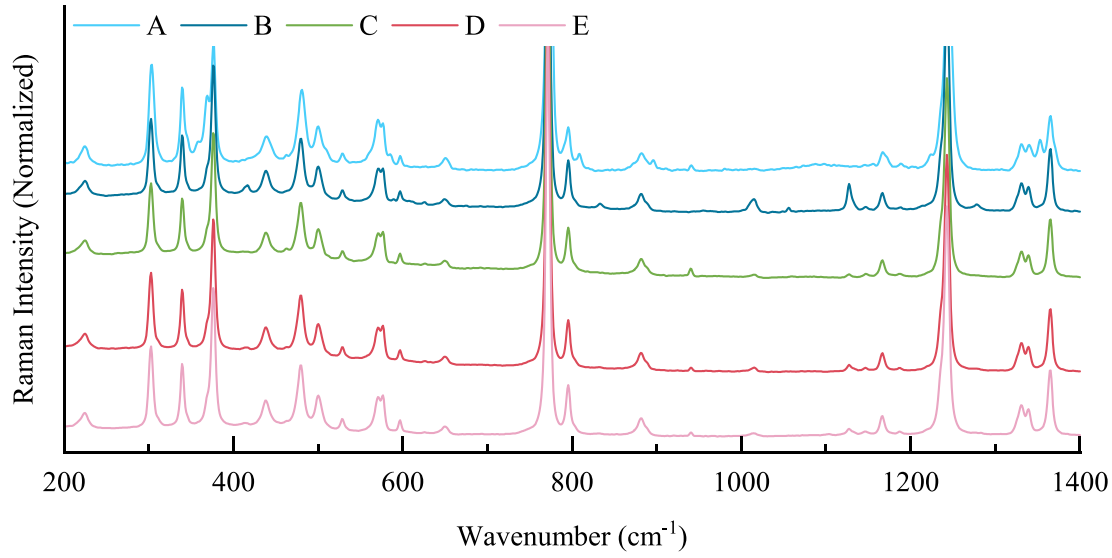

Figure 4. Raman spectra of $Ca(FSI)_2$ salts A–E (top peaks cut for clarity).

3.3. Spectroscopic assessment of salt purity

The Raman spectra of the five $Ca(FSI)_2$ salts are very similar at large, with the most notable differences obtained for salt A, which is missing the bands at 1015, 1127, and 1147 cm^{-1}, present, albeit weak, in the other salts (figure 4). The two former bands are particularly strong in the spectrum of salt B, which also shows bands at 833, 1055, and 1278 cm^{-1}, which are not present in any of the other salts. We truly do not believe our drying has affected any salts in any fundamentally problematic way, but we note that the band at 1055 cm^{-1} differs in the Raman spectra of pristine vs dried salt B (Figure S2). Unique stand-alone bands are typically associated with the presence of a different compound; altogether, the spectra indicates that salt A has the highest purity and salt B the lowest (in accordance with the thermal analysis results). Salt A, however, distinguishes itself as the only salt with several additional shoulders at 359, 369, 585, 809, 896, 1225, and 1353 cm^{-1}, which is tentatively attributed to the possibility that $Ca(FSI)_2$ may adopt two different crystal structures. Although there is no published crystallographic data on $Ca(FSI)_2$, the analogous Na-, K-, and CsFSI salts all crystallize in two or more distinct structures [27]. An extensive band assignment is provided in table S1 [25, 28, 29]

Moving to the IR spectra (figure S3), these appear nearly identical, but minor differences can still be observed. In particular, looking at the region 630–700 cm^{-1} (figure 5), all salts have a weak but clear band at 653 cm^{-1} (δ SNS), but the more or less equally weak band at 673 cm^{-1} is only found for salts C and E, and slightly differently positioned, at 677 cm^{-1}, for salts B and D, and almost not present at all in the spectrum of salt A. Furthermore, while all salts show a large shoulder area between 1050 and 1225 cm^{-1}, a third band breaks out more visibly in the spectra of salts D and E. Again, taken altogether, this points to salt A to be the purest salt.

3.4. Electrochemical performance

In stark contrast to the many and noticeable differences above between salts A–E, the Ca|0.1 M $Ca(FSI)_2$ in DMAc |PTCDI full cells all show similar discharge capacities (figures 6 and S4). Here, the cell using the electrolyte based on salt B shows only marginally worse discharge capacity as well as a higher overpotential upon charging. It should be stressed that there are really no readily available cathodes that can truly challenge the electrolyte's high-voltage stability and thus test these rather subtle salt differences. Therefore, symmetric Ca||Ca cells are employed to assess differences in long-term cycling behavior, noting that any problems observed in symmetric cells will certainly be amplified in more complex and real cell configurations.

Initially, all symmetric cells have a stable overpotential of $\pm$1.15 V, which is kept until 250 h, at which the polarization of cell B steadily increases until complete failure (at 457 h) (figure 7(a)). Slightly before that event, cells C and D also increase in polarization, and slightly after that, cell A as well. Overall, cell E maintains the lowest polarization the longest, but then rapidly increases, and, in agreement with all the above observations, cell A delivers the most stable cycling. Moving to the rate capability tests (figure 7(b)), there are no significant differences between the cells.

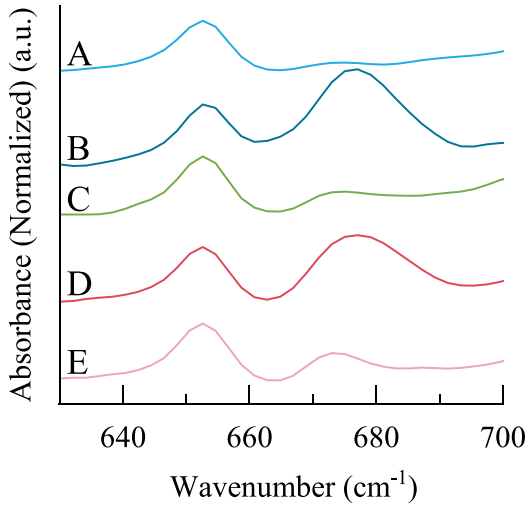

Figure 5. FTIR spectra of $Ca(FSI)_2$ salts (A)–(E) in the region 630–700 cm^{-1}.

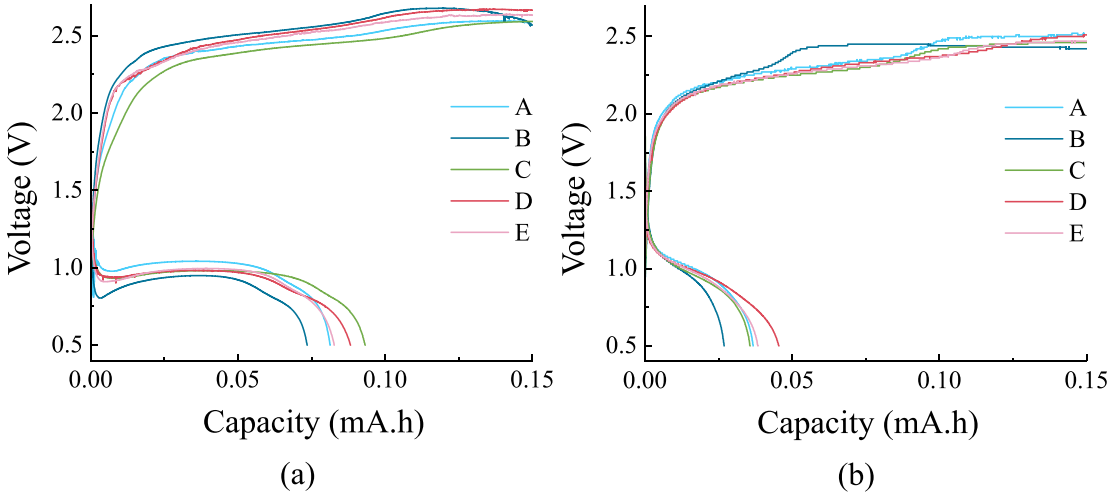

Figure 6. Voltage profiles of Ca|0.1 M $Ca(FSI)_2$ in DMAc|PTCDI full cells at: (a) cycle 2 and (b) cycle 7.

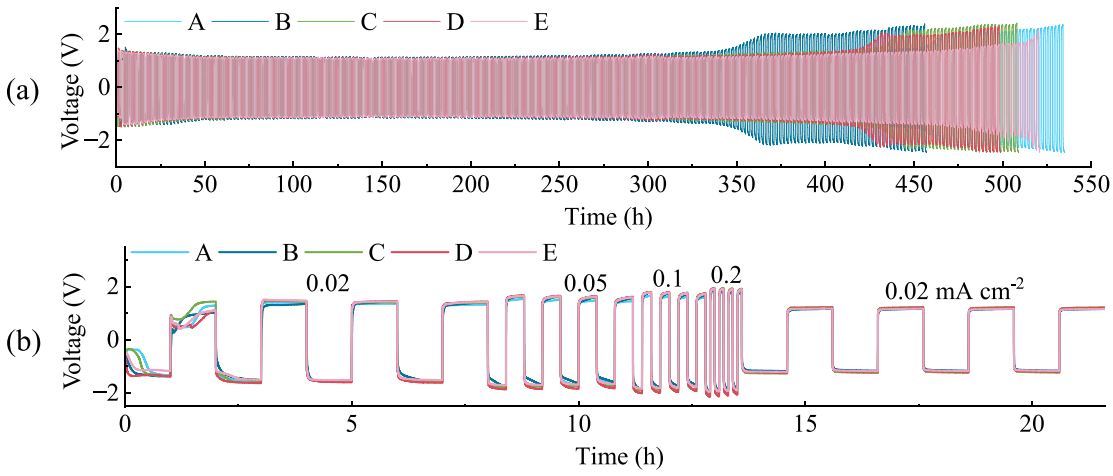

Figure 7. (a) Long-term cycling and (b) rate capability tests of Ca|0.1 M $Ca(FSI)_2$ in DMAc|Ca cells.

4. Conclusions

Ten years ago, it was found that one of the three commercially available LiFSI salts contained some contamination [25]. This time, the purity differences found for the five $Ca(FSI)_2$ salts are even more apparent. Whereas salt B had the most significant differences, most obviously in macroscopic appearance but perhaps also related to impurities and even its crystal structure, as compared to the other salts, and also performs the worst, none of the other salts show identical/similar properties or performances to one another. This is alarming, as regardless of the supplier, the same salt should yield the same psycho-chemical properties, and learnings from a decade more of LiFSI synthesis know-how should from our perspective, perhaps naïvely, be accordingly reflected. Finally, it is particularly concerning that this demands that anyone working on CaB development—which is still in its infancy and heavily reliant on establishing a 'standard electrolyte' for cathode and full cell evaluation—must in parallel resort to do both basic physico-chemical characterization of the salt employed as well as taking into consideration that the electrochemical performance might depend on the salt used in the electrolyte. We unfortunately do not believe this to be limited to the here investigated $Ca(FSI)_2$ salts, nor to Ca-salts for that matter—which is why we call for caution when working within NGB R&D and using commercially sourced materials.

Acknowledgments

J.T. is grateful to Dr Zaher Slim for providing the PTCDI cathodes and to Dr Patricia Huijbers for valuable feedback on the first draft of the manuscript. The authors would also like to gratefully acknowledge the financial support from the Swedish Research Council (Grants #2020–03988 and #2021–00613).

Data availability statement

The data cannot be made publicly available upon publication because they contain commercially sensitive information. The data that support the findings of this study are available upon reasonable request from the authors.

$Ca(FSI)_2$ salt additional data available at https://doi.org/10.1088/2515-7655/ae5453/data1.

ORCID iDs

Johanna Timhagen 0009-0008-5844-4524
Patrik Johansson 0000-0002-9907-117X

References

[1] Cao Y, Li M, Lu J, Liu J and Amine K 2019 Bridging the academic and industrial metrics for next-generation practical batteries *Nat. Nanotechnol.* **14** 200–7
[2] Yu X and Manthiram A 2021 Sustainable battery materials for next-generation electrical energy storage *Adv. Energy Sustain. Res.* **2** 2000102
[3] Meng Y S, Srinivasan V and Xu K 2022 Designing better electrolytes *Science* **378** 1–8
[4] Ji B, He H, Yao W and Tang Y 2021 Recent advances and perspectives on calcium-ion storage: key materials and devices *Adv. Mater.* **33** 2005501
[5] Song H and Wang C 2022 Current status and challenges of calcium metal batteries *Adv. Energy Sustain. Res.* **3** 2100192
[6] Arroyo-De Dompablo M E, Ponrouch A, Johansson P and Palacín M R 2020 Achievements, challenges, and prospects of calcium batteries *Chem. Rev.* **120** 6331–57
[7] Monti D, Ponrouch A, Araujo R B, Barde F, Johansson P and Palacín M R 2019 Multivalent batteries-prospects for high energy density: Ca batteries *Front. Chem.* **7** 79
[8] Forero-Saboya J, Davoisne C, Dedryvère R, Yousef I, Canepa P and Ponrouch A 2020 Understanding the nature of the passivation layer enabling reversible calcium plating *Energy Environ. Sci.* **13** 3423–31
[9] Ponrouch A, Frontera C, Bardé F and Palacín M R 2016 Towards a calcium-based rechargeable battery *Nat. Mater.* **15** 169–72
[10] Forero-Saboya J D, Lozinšek M and Ponrouch A 2020 Towards dry and contaminant free $Ca(BF_4)_2$-based electrolytes for Ca plating *J. Power Sources Adv.* **6** 100032
[11] Li Z, Fuhr O, Fichtner M and Zhao-Karger Z 2019 Towards stable and efficient electrolytes for room-temperature rechargeable calcium batteries *Energy Environ. Sci.* **12** 3496–501
[12] Shyamsunder A, Blanc L E, Assoud A and Nazar L F 2019 Reversible calcium plating and stripping at room temperature using a borate salt *ACS Energy Lett.* **4** 2271–6

[13] Nielson K V, Luo J and Liu T L 2020 Optimizing calcium electrolytes by solvent manipulation for calcium batteries *Batter. Supercaps* **3** 766–72
[14] Yi Y *et al* 2024 Deciphering anion-modulated solvation structure for calcium intercalation into graphite for Ca-Ion batteries *Angew. Chem. Int. Ed.* **63** e202317177
[15] Cai Y, Zhang H, Cao Y, Wang Q, Cao B, Zhou Z, Lv F, Song W, Duo D and Yu L 2022 Application and industrialization of LiFSI: a review and perspective *J. Power Sources* **535** 231481
[16] Han H B, Zhou S-S, Zhang D-J, Feng S-W, Li L-F, Liu K, Feng W-F, Nie J, Li H and Huang X-J 2011 Lithium bis(fluorosulfonyl)imide (LiFSI) as conducting salt for nonaqueous liquid electrolytes for lithium-ion batteries: physicochemical and electrochemical properties *J. Power Sources* **196** 3623–32
[17] Timhagen J, Cruz C, Weidow J and Johansson P 2024 Local structure and entropic stabilization of Ca-based molten salt electrolytes *Batter. Supercaps* **7** e202400297
[18] Li J, Han C, Ou X and Tang Y 2022 Concentrated electrolyte for high-performance Ca-Ion battery based on organic anode and graphite cathode *Angew. Chem. Int. Ed.* **61** e202116668
[19] Zhou R, Hou Z, Fan K, Wun C K, Liu Q, Benedict Lo T W, Huang H and Zhang B 2023 An advanced organic cathode for non-aqueous and aqueous calcium-based dual ion batteries *J. Power Sources* **569** 232995
[20] Hou Z, Zhou R, Yao Y, Min Z, Lu Z, Zhu Y, Tarascon J M and Zhang B 2022 Correlation between electrolyte chemistry and solid electrolyte interphase for reversible Ca metal anodes *Angew. Chem. Int. Ed.* **61** e202214796
[21] Hou Z, Zhou R, Min Z, Lu Z and Zhang B 2023 Realizing wide-temperature reversible Ca metal anodes through a Ca^{2+}-conducting artificial layer *ACS Energy Lett.* **8** 274–9
[22] Slim Z, Cruz-Cardona C, Pechberty C, Hosaka T, Mandić Z, Panic V and Johansson P 2025 Solvent-mediated electrolyte design for calcium metal batteries *ACS Mater. Lett.* **7** 3235–42
[23] Ye L *et al* 2024 A rechargeable calcium–oxygen battery that operates at room temperature *Nature* **626** 313–8
[24] Hahn N T, McClary S A, Landers A T and Zavadil K R 2022 Efficacy of stabilizing calcium battery electrolytes through salt-directed coordination change *J. Phys. Chem. C* **126** 10335–45
[25] Kerner M, Plylahan N, Scheers J and Johansson P 2016 Thermal stability and decomposition of lithium bis(fluorosulfonyl)imide (LiFSI) salts *RSC Adv.* **6** 23327–34
[26] Huang J and Hollenkamp A F 2010 Thermal behavior of ionic liquids containing the FSI anion and the Li^+ cation *J. Phys. Chem. C* **114** 21840–7
[27] Matsumoto K, Oka T, Nohira T and Hagiwara R 2013 Polymorphism of alkali bis(fluorosulfonyl)amides ($M[N(SO_2F)_2]$, M = Na, K, and Cs) *Inorg. Chem.* **52** 568–76
[28] Li L, Zhou S, Han H, Li H, Nie J, Armand M, Zhou Z and Huang X 2011 Transport and electrochemical properties and spectral features of non-aqueous electrolytes containing LiFSI in linear carbonate solvents *J. Electrochem. Soc.* **158** A74–A82
[29] Scheers J and Johansson P 2012 Comment on "transport and electrochemical properties and spectral features of non-aqueous electrolytes containing LiFSI in linear carbonate solvents" [J. Electrochem. Soc., 158, A74 (2011)] *J. Electrochem. Soc.* **159** S1–S2